Mechanistic Aspects of the Rhodium-Catalyzed Hydrogenation of CO_2 to Formic Acid—A Theoretical and Kinetic Study[†,|]

François Hutschka,[‡] Alain Dedieu,*[,‡] Martin Eichberger,[§] Roland Fornika,[§] and Walter Leitner*[,⊥,§]

Contribution from the Laboratoire de Chimie Quantique, UPR 139 du CNRS, Université Louis Pasteur, 4 rue Blaise Pascal, F-67000 Strasbourg France, Max-Planck-Institut für Kohlenforschung, Kaiser-Wilhelm-Platz 1, D-45470 Mülheim/Ruhr, Germany, and Max-Planck-Gesellschaft, Arbeitsgruppe "CO_2-Chemie" an der Universität Jena, Lessingstrasse 12, D-74430 Jena, Germany

Received May 13, 1996[⊗]

Abstract: The mechanism of the rhodium-catalyzed hydrogenation of CO_2 to formic acid was investigated by initial rate measurements using the complex [(dppp)Rh(hfacac)] (**A**) (dppp = $Ph_2P(CH_2)_3PPh_2$, hfacac = hexafluoroacetylacetonate) as a catalyst precursor in DMSO/NEt_3 and by *ab initio* calculations using *cis*-[$(H_3P)_2Rh$] as a model fragment for the catalytically active site. The kinetic data are consistent with a mechanism that involves rate limiting product formation by liberation of formic acid from an intermediate that is formed *via* two reversible reactions of the actual catalytically active species first with CO_2 and then with H_2. The calculations provide for the first time a theoretical analysis of the full catalytic cycle of CO_2 hydrogenation. They give detailed insight into the structure of possible intermediates and their transformations during the individual steps. The results suggest σ-bond metathesis as an alternative low energy pathway to a classical oxidative addition/reductive elimination sequence for the reaction of the formate intermediate with dihydrogen.

1. Introduction

Activation of carbon dioxide is presently an important field of research in organometallic chemistry, both experimentally[1] and theoretically.[2] Catalytic hydrogenation of CO_2 to formic acid has attracted much interest in recent years as it provides a promising approach to the use of CO_2 as a raw material in large scale chemical synthesis.[3−6] In principle there are various ways in which transition metal centers can catalyze the combination of H_2 with CO_2,[3] but in most of the successful catalytic systems known to date the intimate aspects of the mechanism have not been fully assessed. A detailed picture of the sequence of steps leading to the desired product clearly would facilitate a rational design of potential catalysts.

We have found that rhodium phosphine complexes act as very efficient catalysts for the formation of formic acid from CO_2 in nonprotic polar solvents in the presence of amines.[5,6] On the basis of NMR-spectroscopic investigations of model reactions[7] a mechanism was proposed involving CO_2 insertion into the Rh−H bond followed by a sequence of oxidative addition and reductive elimination steps for the H_2 activation process (path A of Scheme 1).[5b] More recently, we have suggested an alternative pathway for the H_2 cleavage on the basis of ab initio calculations.[8] In this case no change of the oxidation state of the rhodium center is required, and the formation of formic acid is a result of a [2 + 2] addition of H_2 on the rhodium formate intermediate obtained after CO_2 insertion (path B of Scheme 1). We now wish to present a full account of the theoretical

[†] Activation of Carbon Dioxide, 8. For Part 7 see ref 10.

[‡] Université Louis Pasteur. Telefax: Int. code + 3 88 61 20 85. E-mail: dedieu@quantix.u-strasbg.fr.

[§] Arbeitsgruppe "CO_2-Chemie" an der Universität Jena.

[⊥] Max-Planck-Institut für Kohlenforschung. Telefax: Int. code + 208 306 29 80. E-mail: leitner@mpi-muelheim.mpg.de.

[|] Keywords: catalysis; ab initio calculations; carbon dioxide; hydrogenation; rhodium complexes.

[⊗] Abstract published in *Advance ACS Abstracts,* April 1, 1997.

(1) (a) Behr, A. *Carbon Dioxide Activation by Metal Complexes*; VCH: Weinheim, 1988. (b) *Enzymatic and Model Carboxylation and Reduction Reactions for Carbon Dioxide Utilization (NATO ASI Serie C, 314)*; Aresta, M., Schloss, J. V., Eds.; Kluwer Academic Press: Dordrecht, 1990. (c) Dinjus, E.; Fornika, R. Carbon Dioxide as C_1 Building Block. In *Applied Homogeneous Catalysis with Organometallic Compounds, Vol. 2*; Cornils, B., Herrmann, W. A., Eds.; VCH: Weinheim, 1998; pp 1048−1072. (d) Aresta, M.; Quaranta, E.; Tommasi, I.; Giannoccaro, P.; Ciccarese, A. *Gazz. Chim. Ital.* **1995**, *125*, 509. (e) Leitner, W. *Coord. Chem. Rev.* **1996**, *153*, 257. (f) Gibson, D. H. *Chem. Rev.* **1996**, *96*, 2063.

(2) For reviews of theoretical studies on CO_2 coordination in transition metal complexes, see: (a) Sakaki, S.; Dedieu A. *Inorg. Chem.* **1987**, *26*, 3278. (b) Sakaki, S. *Stereochemistry of Organometallic and Inorganic Compounds 4;* Elsevier Science Pub.: Amsterdam, 1990. For theoretical studies on CO_2 insertion reactions, see: (c) Sakaki, S.; Ohkubo, K. *Inorg. Chem.* **1988**, *27*, 2020. (d) Bo, C.; Dedieu, A. *Ibid.* **1989**, *28*, 304. (e) Sakaki, S.; Ohkubo, K. *Organometallics* **1989**, *8*, 2970. (f) Sakaki, S.; Ohkubo, K. *Inorg. Chem.* **1989**, *28*, 2583. (g) Sakaki, S.; Musahi, Y. *J. Chem. Soc., Dalton Trans*. **1994**, 3047. (h) Sakaki, S.; Musahi, Y. *Int. J. Quant. Chem.* **1996**, 57, 481. For theoretical studies on coupling reactions, see: (i) Dedieu, A.; Ingold, F. *Angew. Chem., Int. Ed. Engl.* **1989**, *28*, 1694. (j) Dedieu, A.; Bo, C.; Ingold F. In ref 1b, p 23. (k) Dedieu, A.; Bo, C.; Ingold F. In *Metal-Ligand Interactions; from Atoms to Clusters, to Surfaces*; Salahub, D., Russo, N., Eds.; *NATO ASI Series* 1992; C378, p 175. (l) Sakaki, S.; Mine, K.; Tagushi, D.; Arai T. *Bull. Chem. Soc. Jpn.* **1993**, *66*, 3289.

(3) (a) Jessop, P. G.; Ikariya, T.; Noyori, R. *Chem. Rev.* **1995**, *95* 259. (b) Leitner, W. *Angew. Chem.* **1995**, *107*, 2391; *Angew. Chem., Int. Ed. Engl.* **1995**, *34*, 2207.

(4) (a) Inoue, Y.; Izumida, H.; Sasaki, S.; Hashimoto, H. *Chem. Lett.* **1976**, 863. (b) Taqui Khan, M. M.; Halligudi, S. B.; Shukla S. *J. Mol. Catal.* **1989**, *57*, 47. (c) Tsai, J. C.; Nicholas, K. M. *J. Am. Chem. Soc.* **1992**, *114*, 5117. (d) Gassner, F.; Leitner, W. *J. Chem. Soc., Chem. Commun.* **1993**, 1465. (e) Jessop, P. G.; Ikariya, T.; Noyori, R. *Nature* **1994**, *368*, 231. (f) Lau, C. P.; Chen, Y. Z. *J. Mol. Catal. A: Chem.* **1995**, *101*, 33. (g) Jessop, P. G.; Hsiao, Y.; Ikariya, T.; Noyori, R. *J. Am. Chem. Soc.* **1996**, *118*, 344. (h) Zhang, J. Z.; L;, Z.; Wang, H.; Wang, C. Y. *J. Mol. Catal. A: Chem.* **1996**, *112*, 9.

(5) (a) Graf, E.; Leitner, W. *J. Chem. Soc., Chem. Commun.* **1992**, 623. (b) Leitner, W.; Dinjus, E.; Gassner, F.; *J. Organomet. Chem.* **1994**, *475*, 257. (c) Graf, E.; Leitner, W. *Chem. Ber.* **1996**, *129*, 91.

(6) (a) Fornika, R.; Görls, H.; Seemann, B.; Leitner, W. *J. Chem. Soc., Chem. Commun.* **1995**, 1479. (b) Angermund, K.; Baumann, W.; Dinjus, E.; Fornika, R.; Görls, H.; Kessler, M.; Krüger, C.; Leitner, W.; Lutz, F. *Chem. Eur. J.* **1997**, in press

(7) Burgemeister, T.; Kastner, F.; Leitner, W. *Angew. Chem.* **1993**, *105*, 781; *Angew. Chem., Int. Ed. Engl*. **1993**, *32*, 739.

(8) Hutschka, F.; Dedieu, A.; Leitner, W. *Angew. Chem.* **1995**, *107*, 1905; *Angew. Chem., Int. Ed. Engl.* **1995**, *34*, 1742.

S0002-7863(96)01579-X CCC: $14.00

Scheme 1

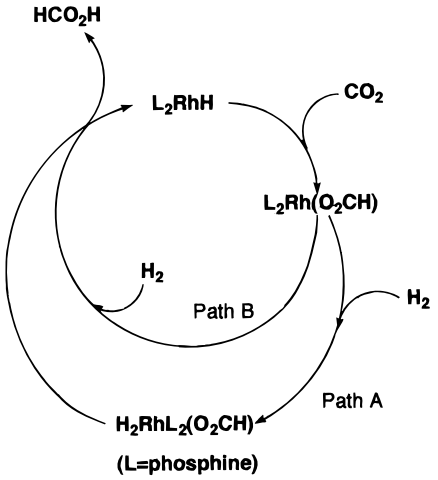

investigation of both pathways together with some new experimental findings that give further insight into the mechanism of this catalytic reaction.

2. Kinetic Investigations of CO_2 Hydrogenation to Formic Acid Using [(dppp)Rh(hfacac)] (A) as the Catalyst Precursor

2.1. Initial Rate Measurements. Complexes of type [(P_2)Rh(hfacac)] (P_2 = chelating bisphosphine ligand, hfacac = hexafluoroacetylacetonate) have been introduced recently as the most effective catalyst precursors for the hydrogenation of CO_2 to formic acid in organic solvents according to eq 1.[6] Complex **A** bearing the phosphorus ligand $Ph_2P(CH_2)_3PPh_2$ (dppp) which forms a six-membered chelate ring at the metal center was chosen in the present investigation as a representative for this type of catalysts, because its medium activity allows changes in the reaction rate to be measured most conveniently.

$$H_2 + CO_2 \xrightarrow[\text{catalyst = A}]{\text{DMSO/NEt}_3\ (5{:}1),\ T = 296\ \text{K}} HCOOH \qquad (1)$$

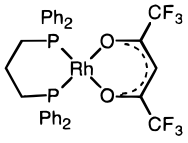

A

A mixture of DMSO and NEt_3 (5:1) was used as a solvent system,[5,6] and Figure 1 shows the concentration/time profile of a typical experiment. The concentration of formic acid increases with maximum rate at the beginning, but the reverse reaction of eq 1 becomes more and more pronounced until an equilibrium concentration of 2.1 M is reached. The final concentration is governed by the influence of the reactions conditions (solvent, temperature, pressure, amine) on the equilibrium constant and hence the Gibbs free energy $\Delta G°$ of eq 1. The high concentration under the given conditions can be attributed mainly to a beneficial effect on the $T\Delta S$ term of $\Delta G°$.[3b,5b]

The kinetics of the forward reaction of eq 1 were investigated by systematic variation of the relevant reaction parameters using the initial rate method (Table 2).[9] The initial rate v_o is defined according to eq 2 and was obtained from linear regression of data points corresponding to less than 10% of the equilibrium concentration (Figure 1, insert). The concentrations of the reaction gases in the solvent system were assumed to be directly proportional to their partial pressures for data analysis. The data presented in Figure 1 were obtained at a concentration of 1.50×10^{-3} M of complex **A** and at partial pressures of 20 and 5 bar for CO_2 and H_2, respectively. They correspond to an initial rate $v_o = 1.57 \times 10^{-4}$ M s^{-1}. The values of v_o were reproducible within ±5% deviation.

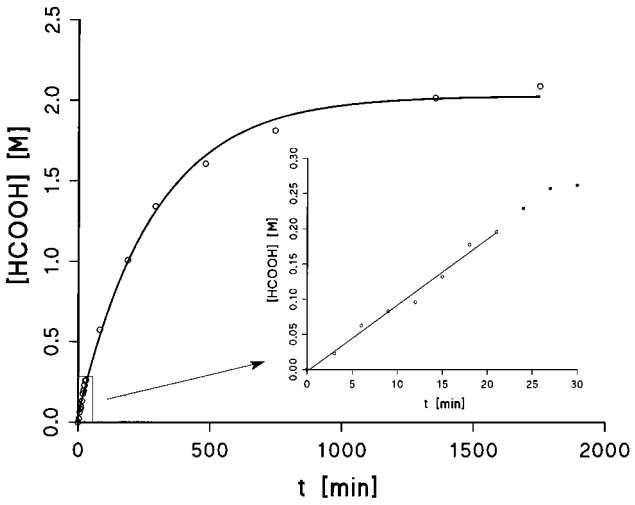

Figure 1. Concentration/time profile and determination of the initial rate v_o for the formation of HCOOH from H_2 and CO_2 catalyzed by [(dppp)Rh(hfacac)] **A**. See text for experimental details.

Table 1. Influence of Catalyst Pretreatment with H_2 or CO_2 on the Initial Rate of Formic Acid Production Using Catalyst Solutions Containing [(dppp)Rh(hfacac)] **A**

	pretreatment with 20 bar		
entry	H_2 [min]	CO_2 [min]	v_o[a] [10^{-4} M s^{-1}]
1			3.05
2	10		3.00
3	20		3.00
4	30		2.73
5	60		2.95
6		10	2.78
7		60	2.25

[a] Reaction conditions: DMSO/NEt_3 (5:1), [**A**] = 2.5×10^{-3}M, $p(H_2)$ = 20 bar, $p(CO_2)$ = 20 bar, T = 296 K.

$$v_0 = (d[\text{HCOOH}]/dt)_{t=0} = k_{obs}[\text{Rh}]^a[\text{H}_2]^b[\text{CO}_2]^c \qquad (2)$$

In earlier studies, the activities of rhodium catalysts formed *in situ* from phosphine free precursor complexes and chelating phosphine ligands have been shown to be highly sensitive to treatment with H_2 or CO_2 *prior* to reaction, H_2 leading to activation while CO_2 deactivated the catalyst.[5b,10] In marked contrast, no significant changes in activity occurred when catalyst solutions containing **A** were stirred under 20 bar of H_2 for periods of up to 60 min before introducing CO_2 (Table 1). Stirring the solution under 20 bar of CO_2 for 60 min lead to a decrease of the initial rate by only 25%, whereas almost complete deactivation is observed with the *in situ* systems under the same conditions.[5b]

A linear relationship between the initial rate of HCOOH production and the concentration of complex **A** was observed in the range of [**A**] = (0.5−4.0) × 10^{-3} M, but no further increase in rate resulted at even higher concentrations (Table 2, Figure 2). A double logarithmic analysis of the data up to [**A**] = 4.0×10^{-3} M according to eq 3 reveals a reaction order of 1.06 (r^2 = 0.996) with respect to rhodium concentration. The

(9) Connors, K. A. *Chemical Kinetics*; VCH: Weinheim, 1990.

(10) Gassner, F.; Dinjus, E.; Görls, H.; Leitner, W. *Organometallics* **1996**, *15*, 2078.

Table 2 . Kinetic Data for the Hydrogenation of CO_2 to Formic Acid Catalyzed by [(dppp)Rh(hfacac)] **A** in DMSO/NEt_3 (5:1, $[NEt_3]_0 = 1.20$ M) at 296 K

entry	[**A**] [10^{-3} M]	$p(CO_2)$ [bar]	$p(H_2)$ [bar]	$[HCOOH]_{eq}$ [M]	v_0 [10^{-4} M s^{-1}]	k'_{obs} [s^{-1}]
1	0.50	20	20	1.50 [a]	0.53	0.107
2	1.00	20	20	1.99 [a]	1.25	0.125
3	1.50	20	20	2.12	1.90	0.127
4	2.50	20	20	2.33	3.05	0.122
5	4.00	20	20		4.95	0.124
6	5.00	20	20	2.21	5.08	0.102
7	1.50	20	2.5	1.66	0.77	
8	1.50	20	5	2.09	1.57	
9	1.50	20	10	2.11	1.78	
10	1.50	20	20	2.13	1.90	
11	1.50	20	30	2.07	2.03	
12	1.50	25	10	1.79[a]	1.85	
13	1.50	30	10	2.59	2.15	
14	1.50	40	10	2.80	2.72	
15	1.50	45	10	3.11	3.12	
16[b]	2.50	20	20	0.96	2.40	
17[c]	2.50	20	20	1.26	4.95	
18[d]	2.50	20	20	0.94	1.23	

[a] Not fully equilibrated. [b] DMSO/NEt_3, $[NEt_3]_0 = 0.60$ M. [c] DMSO/quinuclidine, $[quinuclidine]_0 = 0.60$ M. [d] DMSO/NEt^iPr_2, $[NEt^iPr_2]_0 = 0.60$ M.

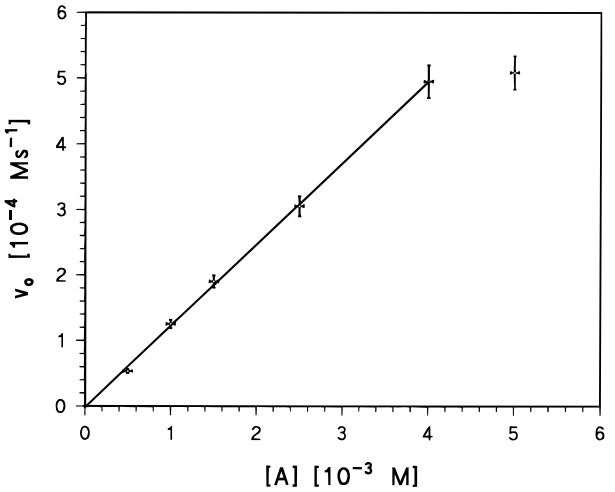

Figure 2. Dependence of the initial rate v_o of the hydrogenation of CO_2 to formic acid catalyzed by [(dppp)Rh(hfacac)] **A** on the total rhodium concentration [**A**]. The solid line was obtained by linear regression for data points [**A**] $< 4.0 \times 10^{-3}$ M.

observable first order rate constant k'_{obs} was determined to (0.121 $\pm$ 0.008) s^{-1} which is equivalent to a turnover frequency of (436 $\pm$ 29) h^{-1} under the given conditions. A formic acid concentration of 1.50 M was reached at a concentration of [**A**] $= 0.5 \times 10^{-3}$ M within 31 h with the catalyst still being active at that point. These data correspond to a total number of turnovers of 3000 which is the maximum reported value for the rhodium catalyzed CO_2 hydrogenation in organic solvents.[3]

$$\log v_0 = a[Rh] + \log k'_{obs} \quad \text{with} \quad k'_{obs} = k_{obs}[H_2]^b[CO_2]^c \quad (3)$$

The dependence of the initial rate on the partial pressure of carbon dioxide in the pressure range of 20−45 bar is summarized in Table 2 and illustrated in Figure 3. A reaction order of 0.71 ($r^2 = 0.953$) results from double logarithmic analysis of the data. However, the data points show a considerable curvature toward a higher reaction order at higher pressure (0.87 between 25 and 45 bar, $r^2 = 0.996$). Experiments at CO_2 pressures below 20 bar were not carried out owing to the two-phasic nature of the solvent system under these conditions.[5b]

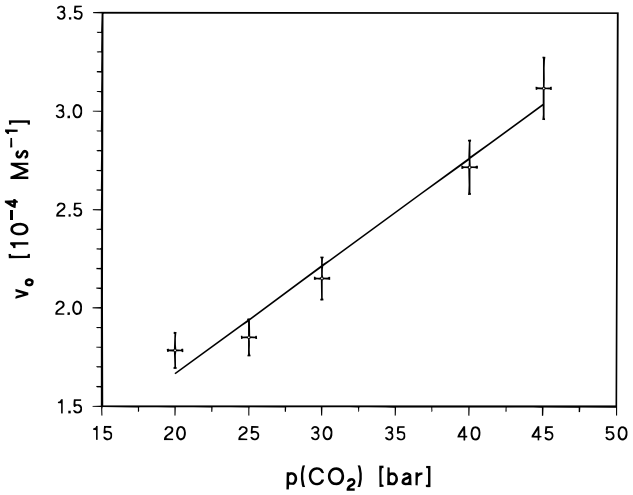

Figure 3. Dependence of the initial rate v_o of the hydrogenation of CO_2 to formic acid catalyzed by [(dppp)Rh(hfacac)] **A** on the initial partial pressure of CO_2. The solid line was obtained by linear regression of all data points.

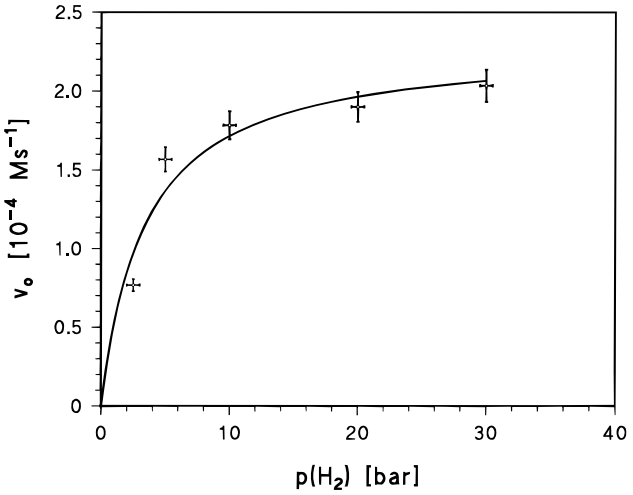

Figure 4. Dependence of the initial rate v_o of the hydrogenation of CO_2 to formic acid catalyzed by [(dppp)Rh(hfacac)] **A** on the initial partial pressure of H_2. The solid line was obtained by iteration using eq 4.

The equilibrium concentration of HCOOH increased steadily with increasing CO_2 pressure from 2.1 to 3.1 M.

A different situation is encountered for the influence of hydrogen pressure on the initial rate. At low pressure, the reaction is cleanly first order in hydrogen, but the rates are practically invariant at hydrogen pressures above 10 bar (Table 2, Figure 4). The data can be described by a hyperbolic function as defined in eq 4 and represented by the solid line in Figure 4 ($r^2 = 0.971$). The final concentration of HCOOH was only affected by hydrogen pressure below 10 bar.

$$v_0 = f\left(\frac{p(H_2)}{1 + p(H_2)}\right) \quad (4)$$

Apart from the concentrations of reactants and catalyst, the amount and the structure of the amine show also significant influence on the reaction rate (Table 2). Replacing NEt_3 from the standard reaction mixture by quinuclidine, a cyclic amine with higher basicity and lower steric demand, leads to an increase in the rate and in the equilibrium concentration. On the other hand, use of bulky and less basic Hünig's base slows down the reaction by a factor of two. The relative solubility

of CO_2 in different reaction mixtures compared to pure DMSO was determined by ^{13}C-NMR spectroscopy under elevated pressure in order to probe for an indirect influence of the amine *via* changes in the CO_2 concentration. The corresponding values were found to be 1.8, 1.3, and 1.4 at identical concentrations of NEt_3, NEt^iPr_2, and quinuclidine, respectively. Thus, the solubility of CO_2 in the system changes with the nature of the amine as expected, but this factor is clearly not the only one responsible for the observed changes in reaction rates.

2.2. Determination of the Rate Law for CO_2 Hydrogenation Catalyzed by A. A plausible kinetic scheme for the mechanism of the rhodium catalyzed hydrogenation of CO_2 that is in agreement with the obtained data and with our earlier NMR spectroscopic investigations[7] is summarized in eqs 5−8.[11] Note, that no assumptions on the exact structures of the intermediates are implied by the given formulas or acronyms (*vide infra*). The catalytic cycle is initiated by hydrogenolysis of the 1,3-diketonate ligand[14] to give a highly unsaturated neutral rhodium hydride $(P_2)RhH$ as the active species. This pathway has been verified experimentally for related complexes $[(P_2)Rh(\eta^3\text{-}C_8H_{13})]$ as catalyst precursors.[10] The intermediate **Rh−1** is then formed from this hydride *via* reversible reaction with CO_2. Subsequently, **Rh−2** is obtained *via* an equilibrium involving H_2 and finally, formic acid is liberated to regenerate the chain carrier $(P_2)RhH$.

$$\underset{\mathbf{A}}{(P_2)Rh(hfacac)} \xrightarrow[-Hhfacac]{+H_2} (P_2)RhH \tag{5}$$

$$(P_2)RhH + CO_2 \underset{k_{-1}}{\overset{k_1}{\rightleftharpoons}} \mathbf{Rh-1} \tag{6}$$

$$\mathbf{Rh-1} + H_2 \underset{k_{-2}}{\overset{k_2}{\rightleftharpoons}} \mathbf{Rh-2} \tag{7}$$

$$\mathbf{Rh-2} \underset{k_{-3}}{\overset{k_3}{\rightleftharpoons}} (P_2)RhH + HCOOH \tag{8}$$

The absence of an induction period and an activating effect of pretreatment with H_2 indicates that the formation of the catalytically active species $(P_2)RhH$ from **A** (eq 5) is fast compared to the actual catalytic cycle. Furthermore, the direct relationship between v_o and [Rh] shows that (i) a constant fraction of **A** is converted into the catalytically active species, (ii) the reaction rate is controlled by the catalytic cycle and not by gas diffusion into the solution, and (iii) the reaction is first order in rhodium. The observation that no further increase of the rate of HCOOH formation occurs at $[\mathbf{A}] > 4.0 \times 10^{-3}$ M can be understood if the overall reaction becomes mass transfer limited at these very high rates. Bimolecular deactivation processes of the catalyst are also possible but might be expected to lead to a gradual decrease rather than a sharp limit of the turnover frequency.

The actual catalytic cycle for CO_2 hydrogenation consists of the steps shown in eqs 6−8, all of them being reversible as required by the reversibility of the overall reaction.[5b] In the initial state of reaction, the concentration of HCOOH can be neglected, and the final step can be regarded as irreversible. The initial rate of appearance of formic acid v_o is then given by eq 9. Under the assumption that the two equilibria are adjusted faster than product formation, this can be rewritten as eq 10. Replacing the unknown concentration of $(P_2)RhH$ by the total rhodium concentration [**A**] using the mass balance (eq 11) leads to the rate law given in eq 12 for the reaction sequence. The factor χ describes the fraction of **A** converted into the active species and may well be 1 in the present case.

$$v_0 = (d[HCOOH]/dt)_{t=0} = k_3[\mathbf{Rh-2}] \tag{9}$$

$$v_0 = k_3K_2K_1[(P_2)RhH][H_2][CO_2] \tag{10}$$

$$\chi[\mathbf{A}] = [(P_2)RhH] + [\mathbf{Rh-1}] + [\mathbf{Rh-2}] \tag{11a}$$

$$\chi[\mathbf{A}] = [(P_2)RhH][1 + K_1[CO_2] + K_2K_1[H_2][CO_2]] \tag{11b}$$

$$v_0 = k_3 \frac{K_2K_1\chi[\mathbf{A}][H_2][CO_2]}{1 + K_1[CO_2] + K_2K_1[H_2][CO_2]} \tag{12}$$

Considering the product forming step rate limiting is strongly supported by the high energy barrier predicted for this process from *ab initio* calculations (*vide infra*). Formic acid liberation has also been proposed to be rate limiting in the mechanism put forward by Nicholas for CO_2 hydrogenation involving less active cationic complexes of rhodium as catalyst precursors.[4c] A stable hydrido rhodium formate complex that does not undergo reductive elimination was described recently by Milstein *et al.*[15] Furthermore, both the reaction with CO_2 and subsequently with H_2 have been shown to occur readily with the catalyst $[(dppp)_2RhH]$, whereas the equilibrium for the product forming step was found to lie considerably to the left.[7] It is also noteworthy in this context, that the influence of the reaction parameters on the equilibrium concentration of formic acids parallels strictly their influence on the initial rates (Table 2). This observation indicates that the overall rate of the forward reaction of eq 1 is much more strongly effected by the investigated parameters than the reverse reaction, for which C−H bond cleavage of coordinated formate has been shown to be the rate limiting step.[16]

The rate law given in eq 12 describes directly the experimentally deduced influence of [**A**] and $p(H_2)$ on v_o. The observed broken reaction order for the dependence of the initial rate v_0 on $p(CO_2)$ indicates that the rates of the first reversible reaction (eq 6) are not fast enough to maintain the equilibrium concentrations on the time scale of the overall reaction. This suggests that—despite the high solubility of CO_2 in the present

(11) (a) We note that our kinetic results do not necessarily rule out an alternative cycle involving a Rh(III) dihydride intermediate $[(P_2)Rh(hfacac)(H)_2]$ as the chain carrier. However, a 18e species seems extremely unlikely to account for the high activity observed with complexes of type **A**. Furthermore, no indication for oxidative addition of H_2 was observed by $^{31}P\{^1H\}$-NMR spectroscopy of a solution of **A** in $[D_6]$DMSO in the presence of excess quinuclidine under 1 atm of H_2 at room temperature.[11b] The signal of **A** ($\delta = 36.9$, d, $J_{RhP} = 183$ Hz) remained unchanged over a period of 2 h. After 18 h, a highly complex $^{31}P\{^1H\}$-spectrum was obtained that could not yet be fully analyzed. A characteristic multiplet centered at $\delta = 125$ indicates the formation of a bridging $RPhP^-$ unit,[12] that might arise from P−Ph bond cleavage of the ligand. Cleavage of P−Ar bonds is frequently observed with highly unsaturated phosphine complexes as intermediates in transition metal catalyzed reactions.[13] (b) Leitner, W., Wittmann, K. Unpublished results.

(12) Carty, A. J.; MacLaughlin, S. A.; Nucciarone, D. In *Phosphorus-31 NMR Spectroscopy in Stereochemical Analysis*; Verkade, J. G., Quin, L. D., Eds.; VCH: Weinheim, 1987; p 559.

(13) (a) Dubois, R. A.; Garrou, P. E.; Lavin, K.; Allock, H. R. *Organometallics* **1984**, *3*, 649. (b) Crabtree, R. H. Organometallic Chemistry of Alkane Activation, In *The Chemistry of Alkanes and Cycloalkanes*; Patai, S., Rappoport, Z., Eds.; Wiley & Sons: Chichester, 1992; p 667 and references therein. (c) Herrmann, W. A.; Kohlpaintner, C. W. *Angew. Chem.* **1993**, *105*, 1588; *Angew. Chem., Int. Ed. Engl.* **1993**, *32*, 1524.

(14) (a) Oswald, A. A.; Hendriksen, D. E.; Kastrup, R. V.; Irikura, K.; Mozeleski, E. J.; Young, D. A. *Phosphorus Sulfur* **1987**, *20*, 237. (b) Moasser, B.; Gladfelter, W. L.; Roe, D. C. *Organometallics* **1995**, *14*, 3832.

(15) Vigalok, A.; Ben-David, Y.; Milstein, D. *Organometallics* **1996**, *15*, 1839.

(16) (a) Strauss, S. H.; Whitmire K. H.; Shriver, D. F. *J. Organomet. Chem.* **1979**, *174*, C59. (b) Leitner, W.; Brown, J. M.; Brunner, H. *J. Am. Chem. Soc.* **1993**, *115*, 152.

Table 3. Total Energies (in hartrees, 1 hartree = 627.7 kcal mol^{-1}) for the Intermediates Involved in the Catalytic Cycle

	MP2/BAE(*)// MP2/BAE(*)	QCISD(T)/BAE(*)// MP2/BAE(*)
CO_2	−188.0136	−188.0288
H_2	−1.1555	−1.1637
trans HCO_2H	−189.1674	−189.1954
cis HCO_2H	−189.1593	−189.1875
1	−5360.8471	−5360.8977
2	−5548.8996	−5548.9581
3	−5548.8928	−5548.9649
4a	−5548.8696	−5548.9509
4b	−5548.8929	−5548.9656
4c	−5548.8880	−5548.9687
4d	−5548.9121	−5548.9911
5a	−5550.0623	−5550.1373
TS 5	−5550.0604	−5550.1352
5c	−5550.0623	
5d	−5550.0728	−5550.1475
5g	−5550.0669	
5h	−5550.0942	
6	−5550.0352	−5550.1081
7	−5550.0521	−5550.1291
8	−5550.0534	−5550.1383
9	−5550.0353	−5550.1147

reaction mixture[5b] and the very low barrier for CO_2 insertion deduced from our calculations (*vide infra*)—the second step (eq 7) is even more facile under the given reaction conditions. In fact, the data represented in Figure 3 can be interpreted as the initial part of an s-shaped rate/concentration profile. Similar curves have been observed for other processes involving two consecutive reversible reactions prior to the rate determining step with the first one being slow compared to the second one.[17]

The reaction sequence outlined in eqs 6−8 provides also a possible explanation for the observation that less sterically demanding and more basic amines lead to higher reaction rates in CO_2 hydrogenation to formic acid. Previous investigations have revealed that the amine component is required to achieve high formic acid yields during the hydrogenation of CO_2 in dipolar nonprotic solvents but that the amine is not a necessary prerequisite for the catalytic cycle to occur.[5b,7] Therefore, the amine has not been included as an integral part of the rate law for the catalytic reaction. However, the presence of a base can be expected to facilitate the liberation of formic acid from the intermediate **Rh**−**2** (eq 8), and the observed amine effects are then fully in line with the assumption that this step is rate limiting.

In conclusion, the kinetic data resulting from the present investigation are in full agreement with the reaction sequence outlined in eqs 5−8. The results are also fully consistent with the catalytic cycle proposed earlier on the basis of NMR investigations.[5b,7] We therefore felt confident to use this catalytic cycle as a basis for a theoretical investigation by *ab initio* calculations of the individual steps and the intermediates involved.

3. Theoretical Study

Ab initio MO/MP2 calculations were carried out on the $[(PH_3)_2RhH] + H_2 + CO_2$ model system using the Gaussian 92 system of programs.[18] Since chelating diphosphine ligands were used in the experiments, a *cis* arrangement of the two PH_3's was imposed. Two different basis sets of valence double-ζ quality were used, but we report here only the calculations carried out with the larger one.[19] This basis set, hereafter denoted as BAE(*), is an all electron basis set supplemented by polarization functions on the C, O, and the H atoms which take part actively in the catalytic process (see the Computational Detail Section). The MP2 optimizations were followed by single point energy calculations carried out at the QCISD(T) level. The shorthand notations MP2//MP2 and QCISD(T)//MP2 will be used to refer to MP2/BAE(*)//MP2/(BAE(*) and QCISD(T)/BAE(*)//MP2/(BAE(*) calculations (following the standard notation "Level of calculation//Level of geometry optimization"). For the corresponding energies of the various structures, see the Computational Detail Section.

3.1. The CO_2 Insertion Step. This step, common to the pathways A and B of the Scheme 1, is shown in Figure 5 with the computed geometries and relative energies of the relevant stationary points. One should mention at the onset that all the calculations reported here refer to singlet states. For most of the systems investigated in this study this is the expected ground state. One might worry about this assumption for **1** and think to a triplet as the ground state, by analogy with findings for *trans*-$[(PH_3)_2RhCl]$.[20] Yet more recent DFT calculations by Margl *et al.*[21] yield the singlet state more stable for the *cis* and the *trans* structure. In **1**, the optimized structure of the singlet state is also found to be more stable than the optimized structure of the triplet state by 16.6 kcal mol^{-1} (MP2//MP2 value). A greater splitting of the d orbitals caused by the greater σ donor character of H compared to Cl may be operating in this case. In line with this reasoning one finds for the $[(PH_3)_2Rh(HCO_2)]$ formate complex—to be discussed later—the singlet more stable than the triplet by only 2.2 kcal mol^{-1}.

Since $[(PH_3)_2RhH]$ is coordinatively unsaturated, one expects that it can easily form a precursor complex with CO_2 by coordination.[1e] The geometry optimization process carried out with the BAE(*) basis set under C_s symmetry constraint led to **2** (see Figure 5). **2** can be described from a structural point of view as a bent η^2-O,C bonded CO_2 complex. The O−C−O angle amounts to 143° and the coordinated CO bond is quite elongated (by 0.08 Å). In order to accommodate the incoming CO_2, both the P−Rh−P and H−Rh−P angles decrease, the effect being more pronounced for the light hydride ligand. Stable Rh complexes containing CO_2 bonded this way have been claimed[22] but not unambiguously characterized[23] until most recently.[15] The computed geometry is indicative of some charge transfer interaction between the doubly occupied Rh dπ orbital and the empty π* orbital of CO_2, in line with a decrease of the population of the dπ orbital from 1.82e in **1** to 1.71e in **2**.

The stabilization energy computed for **2** with respect to **1** + CO_2 is quite substantial (24.4 and 19.8 kcal mol^{-1} at the MP2//MP2 and QCISD(T)//MP2 levels, respectively). It is much larger than the one obtained by Sakaki and Musahi[2g] for the CO_2 insertion into the four-coordinate complex $[(PH_3)_3RhH]$. This is clearly a result of the coordinative unsaturation in the present system $[(PH_3)_2RhH]$.

The geometry of the transition state **3** for the CO_2 insertion is close to the geometry of **2**.[24] It is essentially characterized

(17) Fink, G.; Zoller, W. *Makromol. Chem.* **1981**, *182*, 3265.

(18) *Gaussian 92, Revision E.2.*; Frisch, M. J.; Trucks, G. W.; Head-Gordon, M.; Gill, P. M. W.; Wong, M. W.; Foresman, J. B.; Johnson, B. G.; Schlegel, H. B.; Robb, M. A.; Reploge, E. S.; Gomperts, R.; Andres, J. L.; Raghavachari, K.; Binkley, J. S.; Gonzales, C.; Martin, R. L.; Fox, D. J.; Defrees, D. J.; Baker, J.; Stewart, J. J. P.; Pople, J. A. Gaussian, Inc.: Pittsburgh, PA, 1992.

(19) In our preliminary communication[8] the MP2 geometry optimizations were carried out with the standard LANL1DZ basis (see the Computational Details Section) and were followed by MP2 single point point calculations using the BAE(*) basis set.

(20) Koga, N.; Morokuma, K. *J. Phys. Chem.* **1990**, *94*, 5454.

(21) Margl, P.; Ziegler, T.; Blöchl, P. E. *J. Am. Chem. Soc.* **1995**, *117*, 12625.

(22) Aresta, M.; Nobile, C. F. *Inorg. Chim. Acta* **1977**, *24*, L49.

(23) Dahlenburg, L.; Prengel, C.; Höck, N. *Z. Naturforsch.* **1986**, *41b*, 718 and references therein.

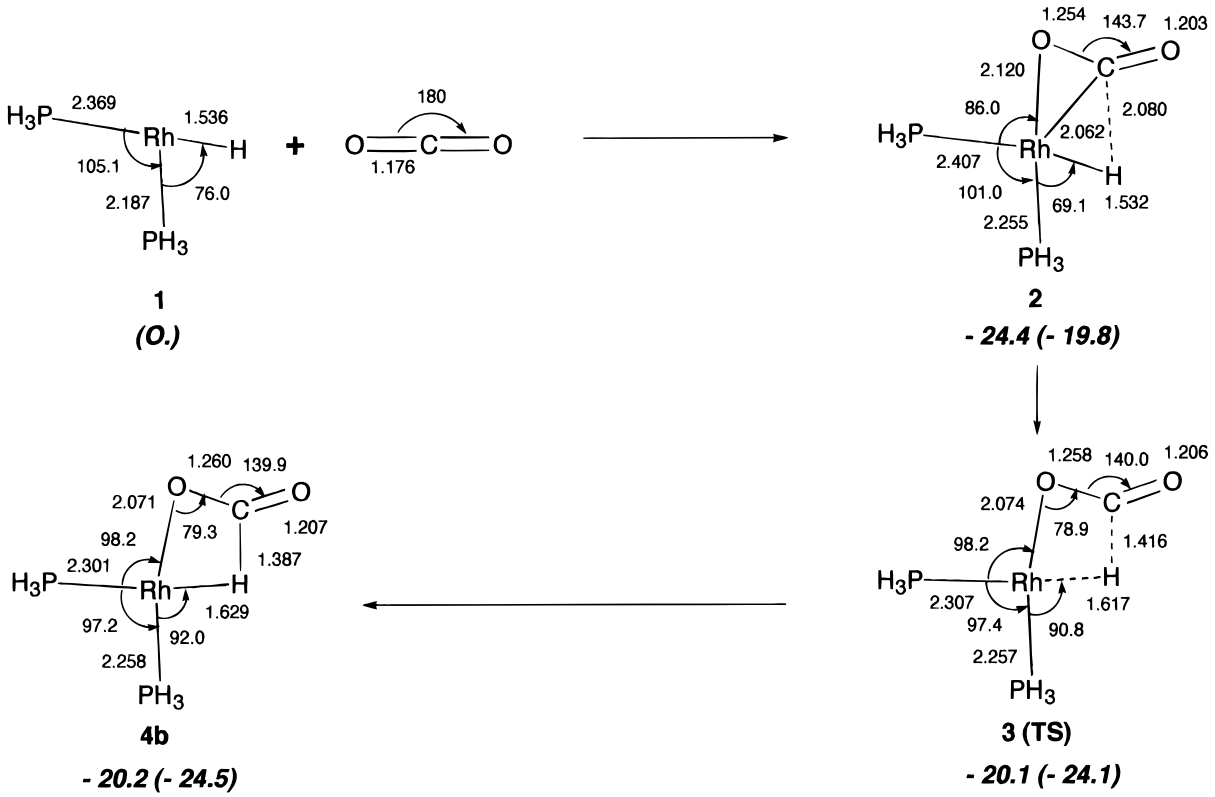

Figure 5. MP2/BAE(*) optimized geometries and relative energies (QCISD(T) values in parentheses) of the structures relevant to the CO_2 insertion into the Rh−H bond of $[(PH_3)_2RhH]$. Bond lengths are in Å and angles in deg. The relative energies are in kcal mol^{-1}.

by the closing of the C−Rh−H angle: the C···H distance decreases from 2.08 to 1.42 Å. This value and the other ones computed for the incipient HCO_2 moiety are very similar to those found by Sakaki and Musahi[2g] for the CO_2 insertion into the Rh−H bond of $[(PH_3)_3RhH]$. The only difference is for the Rh−O bond. Since this bond is already formed in **2** (see above), it does not need to vary further very much: one gets a decrease of only 0.05 Å between **2** and **3**. It is therefore not surprising that the energy barrier to reach the transition state **3** from **2** is appreciably lower: 4.3 kcal mol^{-1} at the MP2//MP2 level, instead of *ca*. 16 kcal mol^{-1} (SD-CI//HF value) for the CO_2 insertion into the Rh−H bond of $[(PH_3)_3RhH]$.[2g] The barrier even disappears when the energy is calculated at the QCISD(T) level, the corresponding QCISD(T)//MP2/value being −4.3 kcal mol^{-1}. This reflects the greater value of the exothermicity computed for the insertion at this level (see Figure 5). Whether or not this negative energy barrier is due to the lack of a geometry optimization performed at the QCISD(T) level cannot be assessed precisely, since a QCISD(T) optimization was not computationally possible. Nevertheless our results indicate clearly that in the gas phase the CO_2 insertion process is rapid and that the barrier, if any, should be low.

There are several possible isomers for the $[(PH_3)_2Rh(HCO_2)]$ system **4**, with either a monohapto or a dihapto coordination mode of the formate ligand. **4a**, **4a′**, and **4b** are the isomers that one can conceive as direct product of the CO_2 insertion. Isomer **4a′** turns out not to be a stable minimum. One gets instead the coordinatively saturated η^2-O,H dihapto complex **4b**, see Figure 5, where both the oxygen and the hydrogen of the formate ligand are bound to the rhodium atom. The geometry of **4b** is very close to the one of the transition state **3**, the greatest difference being for the C−H bond formed during the process: it is 0.03 Å shorter in **4b**. As a result, **4b** lies very close in energy to **3**, being more stable than **3** by only a few tenths of kcal mol^{-1}. Yet the frequency analysis indicates that **4b** is indeed an intermediate.[25]

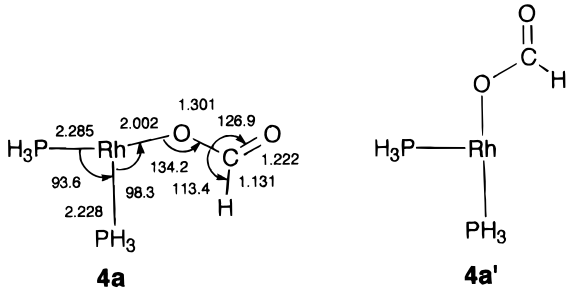

4a is also computed as an equilibrium structure. In fact its structure compares well with the experimental structure of the related $[(PPh_3)_2Rh(CO)(HCO_2)]$ system.[26] However as far as the thermodynamics of the insertion are concerned, **4a** is less stable than the transition state **3** by 14.5 kcal mol^{-1} at the MP2//MP2 level (the energy difference is smaller at the QCISD(T)//MP2 level, 8.8 kcal mol^{-1}). It is therefore likely that **4b** is the isomer that is first obtained in the insertion step, as sketched in Figure 5.

The other possible isomers for the formate intermediate, **4c** and **4d**, cannot result directly from the CO_2 insertion. **4c** is formally obtained from **4a** through a rotation of the OCH moiety

(24) The transition state was characterized in the frequency analysis by an imaginary frequency of 115*i* cm^{-1} with an eigenvector corresponding to the insertion. Another imaginary frequency of 31*i* cm^{-1}corresponding to small displacements of the hydrogens of the PH_3 out of the imposed C_s symmetry plane was obtained. However, the very low values indicate that the C_s restriction is not a severe one and that these frequencies would disappear upon a very slight move from the C_s symmetry, thus leaving only one imaginary frequency.

(25) We only found a very small imaginary frequency of 32*i* cm^{-1} of A″ symmetry corresponding to a rotation of the hydrogens of one phosphine ligand. Thus as far as the insertion is concerned **4b** is a true intermediate.

(26) Grushin, V. V.; Kuznetsov, V. F.; Bensimon, C.; Alper, H. *Organometallics* **1995**, *14*, 3927.

around the C−O bond. It is more stable than **4a** by 11.5 kcal mol^{-1} but less stable than **4b** by 3.1 kcal mol^{-1} (MP2//MP2 values). We have not computed the transition state for the rotation of the formate ligand but a calculation in which the OCH end is rotated by 90° yields an upper limit of 4.3 kcal mol^{-1}. The dihapto η^2-O,O structure **4d** is obtained either from **4a** through an inversion at the coordinated oxygen atom or from **4c** through a rotation of the formate ligand around the Rh−O bond. Not surprisingly, **4d** is found to be the most stable structure of all formate intermediates, being more stable than **4b** by 12.1 kcal mol^{-1}. This high stability results from the achievement of a energetically favored square planar 16 electron species containing two strong rhodium−oxygen bonds. As a result one can reasonably expect[27] that **4d** will not lead to productive channels of the catalytic cycle.

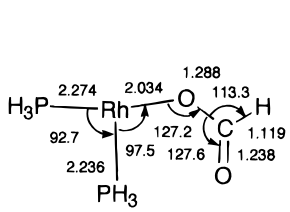

4c

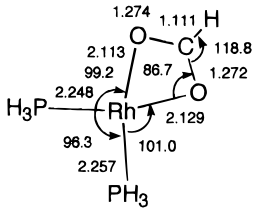

4d

3.2. The Pathway A. The Oxidative Addition of H_2 to the Formate Complex. For the addition of H_2 to **4b** the Rh−H bond turned out to be very weak. All our MP2 geometry optimization searches for the transition state did not retain the dihapto O,H coordination of the formate ligand and the Rh−H bond was cleaved. Thus the overall process corresponds to the addition of H_2 to the three-coordinate formate intermediate **4a** which was therefore used as a starting point for further calculations. In that context one should note that the oxidative addition of H−H, C−H, and Si−H bonds has been shown experimentally[28,29] and theoretically[30] to occur more readily on 14e Rh(I) complexes than on corresponding 16e analogues.

Despite several attempts of various sort, no stable dihydrogen precursor complex corresponding to the oxidative addition of H_2 could be found: The geometry optimization attempts always converged to the cis dihydrido formate product **5a**. Similarly the transition state search did not yield a structure corresponding to the oxidative addition. Instead the computed structure **TS5** and the corresponding imaginary frequency were characteristic of a transition state for the exchange between **5a** and its enantiomer.

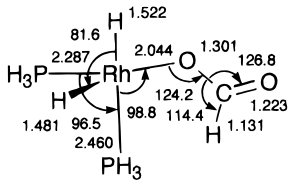

5a

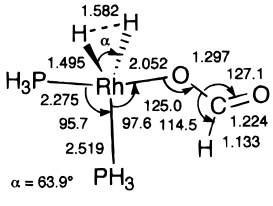

TS 5

Thus, we can conclude from the calculations that the oxidative addition proceeds, at least in the gas phase, without any energy barrier, similar to the result of MP2 calculations by Musaev and Morokuma for the addition of H_2 to [CpRh(CO)].[31] Among the second row transition metals, Rh has also been found to be intrinsically a very effective metal in H_2 oxidative addition.[32] The present oxidative reaction is exothermic: **5a** is more stable than **4b** + H_2 by 8.7 and 5.0 kcal mol^{-1} at the MP2//MP2 and QCISD(T)//MP2 levels, respectively. The decrease of the exothermicity on going from MP2 to QCISD(T) was expected since this has already been noticed by others, *e.g.*, for the oxidative addition of CH_4 to [$(PH_3)_2$RhCl] or to [CpRh(CO)].[33]

5a has a square pyramidal (SP) geometry with an apical hydride, as expected for a strong σ donor ligand in a d^6 transition metal complex.[34,35] It has many rotational isomers, **5b**−**h**, which correspond to a rotation of the formate ligand around

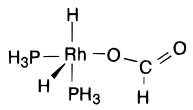

5a
(0.)

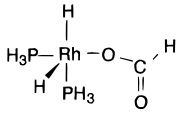

5b

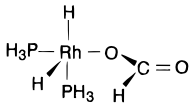

5c
(0.0)

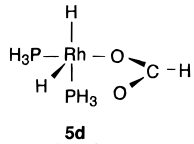

5d
(- 6.6)

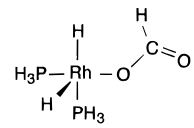

5e

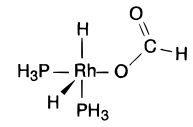

5f

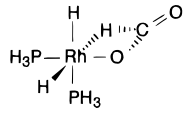

5g
(- 2.9)

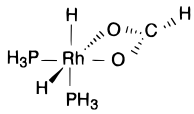

5h
(-20.0)

the Rh−O bond, and for each of these to a rotation of the CHO moiety around the O_{Rh}−C bond. Pilot calculations have shown that such rotations are facile; they do not require more than a few kcal mol^{-1}. Thus isomers which are more stable than the primary product of the oxidative addition **5a** can easily be reached. In order to be *catalytically active* they have to fulfill the following requirements: (i) a planar metal complex must be recovered at the end of the catalytic cycle; (ii) the hydrogen atom and the formate ligand that couple in the reductive elimination of HCO_2H need to be coplanar; and (iii) they should be of moderate stability.[27] These three features are best met by **5c**, **5d**, and **5g** which have a *mer* arrangement of the three spectator ligands (the two phosphine and the hydride that does not eliminate) and are more stable than **5a** by only 3−7 kcal mol^{-1} (MP2//MP2 values).

The coordinatively saturated η^2-O,O dihapto isomer **5h** (which also fulfills the first two requirements) is of course the most stable Rh(III) dihydrido formate complex. This high stability makes it very unlikely to be catalytically productive:

(27) An ideal catalyst avoids too stable intermediates: Albery, W. J.; Knowles, J. R. *Angew. Chem.*, **1977**, *89*, 295; *Angew. Chem., Int. Ed. Engl.* **1977**, *16*, 285.

(28) Duckett, S. B.; Eisenberg, R. *J. Am. Chem. Soc.* **1993**, *111*, 5292.

(29) Hofmann, P.; Meier, C.; Hiller, W.; Heckel, M.; Riede, J.; Schmidt, M. U. *J. Organomet. Chem.* **1995**, *490*, 51.

(30) Musaev, D. G.; Morokuma, K. *J. Organomet. Chem.* **1995**, *504*, 93.

(31) Musaev, D. G.; Morokuma, K. *J. Am. Chem. Soc.* **1995**, *117*, 799.

(32) Siegbahn, P.; Blomberg, M. In *Theoretical Aspects of Homogeneous Catalysis*; van Leeuwen, P. W. N. M., Morokuma, K., van Lenthe J. H., Eds.; Kluwer: Dordrecht, 1995; p 15.

(33) (a) Koga, N.; Morokuma, K. *J. Am. Chem. Soc.* **1993**, *115*, 6883. (b) Couty, M.; Bayse, C. A.; Jiménez-Cataño, R.; Hall, M. B. *J. Phys. Chem.* **1996**, *100*, 13976.

(34) Rossi, A.; Hoffmann, R. *Inorg. Chem.* **1975**, *14*, 365.

(35) Two other isomers for the dihydride complex, a trigonal bipyramid (TBP) structure with two equatorial Rh−H bonds, and a square pyramid structure having two trans hydrides in the basal plane and an apical phosphine ligand were also checked. A C_s constrained geometry optimization starting from a TPB geometry led to the **TS5** structure. Another C_s constrained geometry optimization led to a square pyramid with two basal trans hydrides but much higher in energy than **4b** + H_2. It cannot be a product of the oxidative addition.

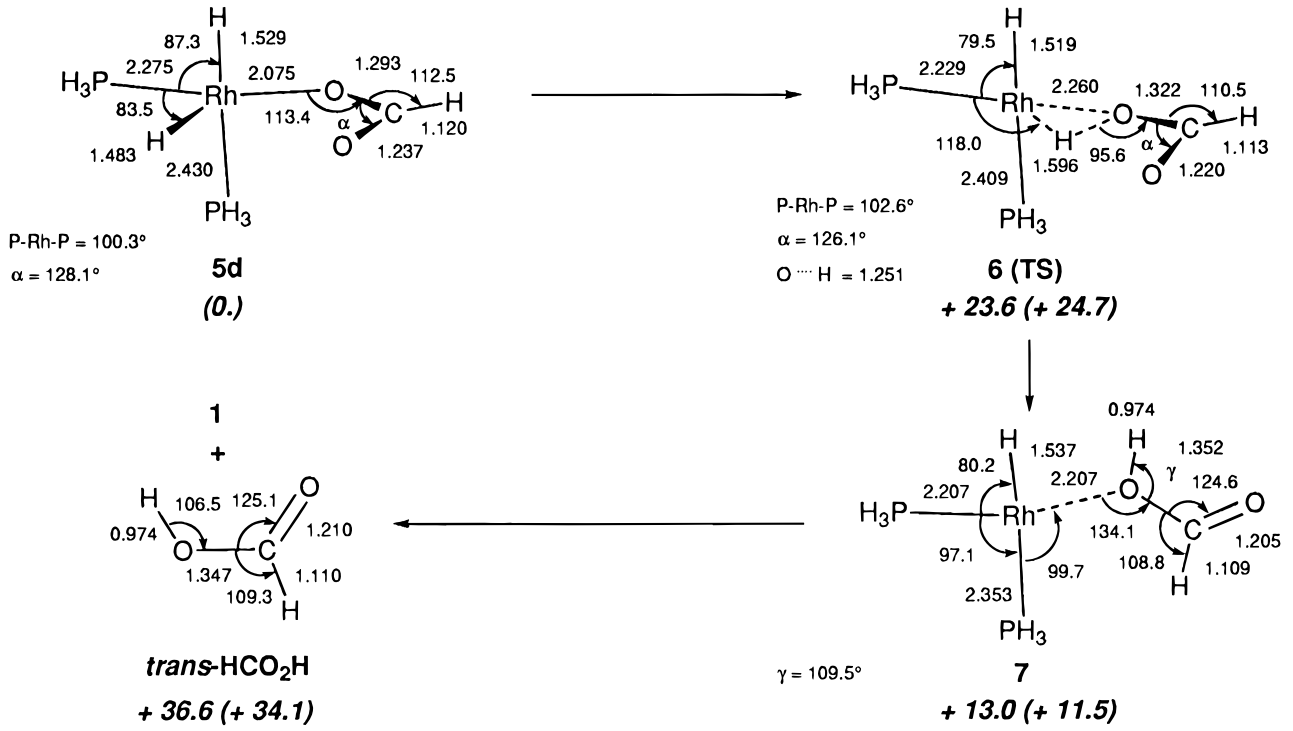

Figure 6. MP2/BAE(*) optimized geometries and relative energies (QCISD(T) values in parentheses) of the structures relevant to the reductive elimination of HCO_2H from $[(PH_3)_2Rh(H)_2(HCO_2)]$. Bond lengths are in Å and angles in deg. The relative energies are in kcal mol^{-1}.

The substantial endothermicity (*vide infra*) of the reductive elimination of formic acid would increase further by at least 13.4 kcal mol^{-1} compared to the reductive elimination from the monohapto formate complexes. Similar considerations have been used by Tsai and Nicholas[4c] to rationalize their experimental observations that Rh(III) dihydrido formate intermediates with a bidendate HCO_2 ligand are unproductive shunts during the hydrogenation of CO_2 using $[Rh(nbd)(PMe_2Ph)_3](BF_4)$ as the catalyst precursor.

The Reductive Elimination of Formic Acid from the Dihydrido Formate Intermediate. Since **5c**, **5d**, and **5g** are within the same energy range we looked at the reductive elimination from these three structures. **5c** and **5g** lead to *cis* formic acid, whereas **5d** leads to the more stable *trans* isomer. In fact one gets first an intermediate complex, $[(PH_3)_2Rh(H)(HCO_2H)]$, in which the formic acid (either *cis* or *trans*) is bound to $[(PH_3)_2RhH]$ through the lone pair of the OH group. The three barrier heights are similar and quite high, ranging between 22 and 24 kcal mol^{-1}. The energies of the $[(PH_3)_2Rh(H)(cis\text{-}HCO_2H)]$ and $[(PH_3)_2Rh(H)(trans\text{-}HCO_2H)]$ intermediates are also quite similar (they lie within 1 kcal mol^{-1}). Thus we report here only the structures corresponding to the elimination of the *trans* formic acid, *viz.* the dihydrido formate complex **5d**, the transition state **6**, and the formic acid complex **7.** They are shown on Figure 6 together with their relative energies. The optimized geometrical parameters of **6** point to a transition state lying on the product side, the O···H distance being short (1.251 Å). Note that in **7** the formic acid lies in the $RhHP_2$ plane. This results from a favorable electrostatic interaction between the hydride and the proton of the OH group. **7** is more stable than the the transition state **6** by about 13 kcal mol^{-1}. The most salient feature is its large stabilization (about 23 kcal mol^{-1}, see Figure 6[36]) with respect to the separated $[(PH_3)_2RhH]$ and ($trans$-HCO_2H) systems.

3.3. The pathway B. The sequence of steps involved in pathway B is shown in Figure 7 together with the relative energies of the corresponding intermediates and transition states. In this route there is no need to invoke a sequence of oxidative addition and reductive elimination. Formic acid is instead obtained through a [2 + 2] metathesis reaction between H_2 and a formate intermediate.

The first step is the approach of H_2 to give the planar dihydrogen complex **8**, see Figure 7.[37] The dihydrogen ligand in **8** is only slightly elongated with respect to free H_2 (0.798 Å instead of 0.738 Å in free H_2) and by relatively short and equivalent Rh−H distances, 1.804 and 1.790 Å. A similar geometry has been optimized for the $[(PH_3)_2(H_2)Pt(H)]$ system.[38] Note also the relatively small angle between the adjacent Rh−H and Rh−O bonds (around 68°). We consider this as an indication of the propensity of the dihydrogen complex system to undergo the [2 + 2] metathesis reaction. **8** is more stable than **4b** + H_2 by 3.2 kcal mol^{-1} at the MP2 level and by 5.7 kcal mol^{-1} at the QCISD(T) level, see Figure 7.

The most interesting aspect of this pathway is the existence of a low energy transition state **9** corresponding to a [2s + 2s] metathesis reaction between H_2 and $[(PH_3)_2Rh(HCO_2)]$.[39] Chart 1 displays the eigenvector corresponding to the imaginary frequency of 1136*i* cm^{-1}. **9** is characterized by an appreciable elongation of the H−H bond from 0.798 Å to 1.103 Å. The computed energy barrier is moderate, whatever the level of the calculation is: 11.4 kcal mol^{-1} at the MP2//MP2 level and 14.8 kcal mol^{-1} at the QCISD(T)//MP2 level.[41,42] This strengthens our proposal about the feasibility of such a pathway.[43] The

(36) One gets a value of 27.1 kcal mol^{-1} for the *cis* systems.

(37) When the geometry optimization was carried out without C_s symmetry constraint, H_2 moved out of the molecular plane by 0.002° only.

(38) Gusev, D. G.; Notheis, J. U.; Rambo, J. R.; Hauger, B. E.; Eisenstein, O.; Caulton, K. G. *J. Am. Chem. Soc.* **1994**, *116*, 7409.

(39) The imaginary frequency amounts to 1136*i* cm^{-1}. Two residual frequencies of 80*i* and 29*i* cm^{-1} corresponding to departure from C_s symmetry by rotation of the PH_3 hydrogens were also found. Again a very slight move from the C_s symmetry should leave only one imaginary frequency.[40]

(40) Cundari, T. R. *J. Am. Chem. Soc.* **1992**, *114*, 10557.

(41) Our preliminary calculations[8] yielded a value of 12.9 kcal mol^{-1}, *i.e.,* in the range of the present values.

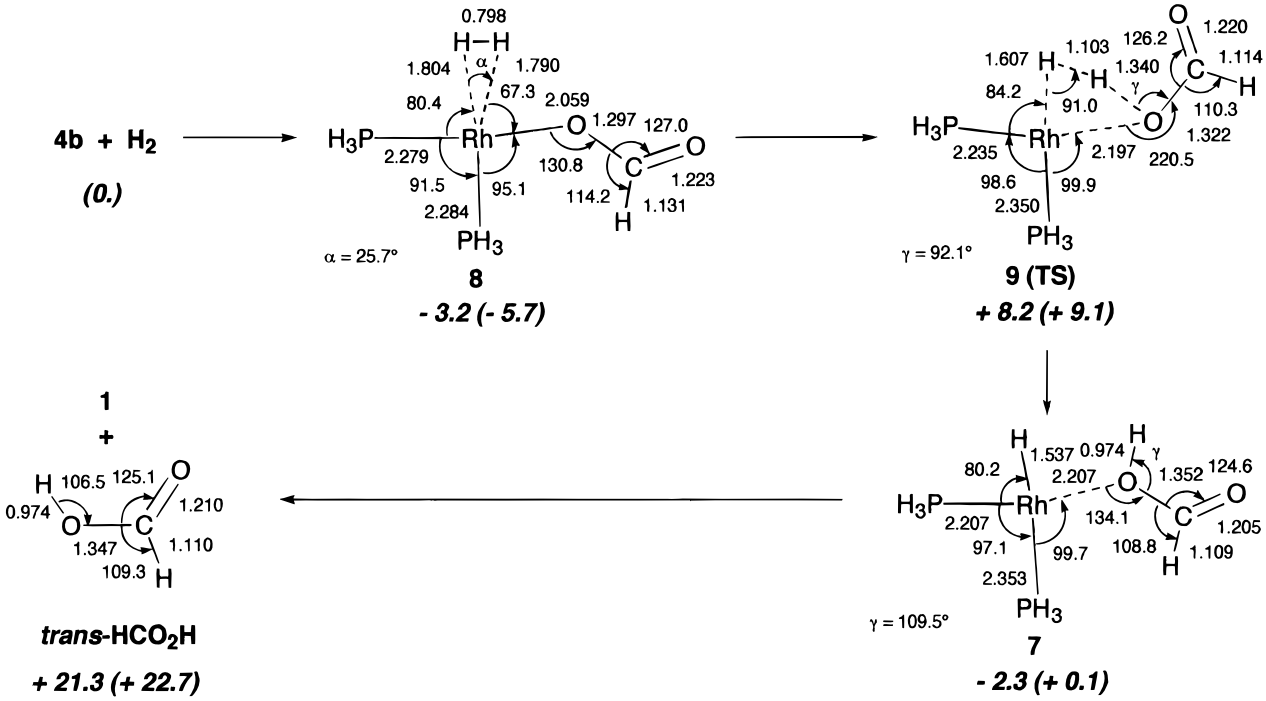

Figure 7. MP2/BAE(*) optimized geometries and relative energies (QCISD(T) values in parentheses) of the structures relevant to the formation of *trans*-HCO_2H through the metathesis reaction of H_2 with $[(PH_3)_2Rh(HCO_2)]$. Bond lengths are in Å and angles in deg. The relative energies are in kcal mol^{-1}.

Chart 1

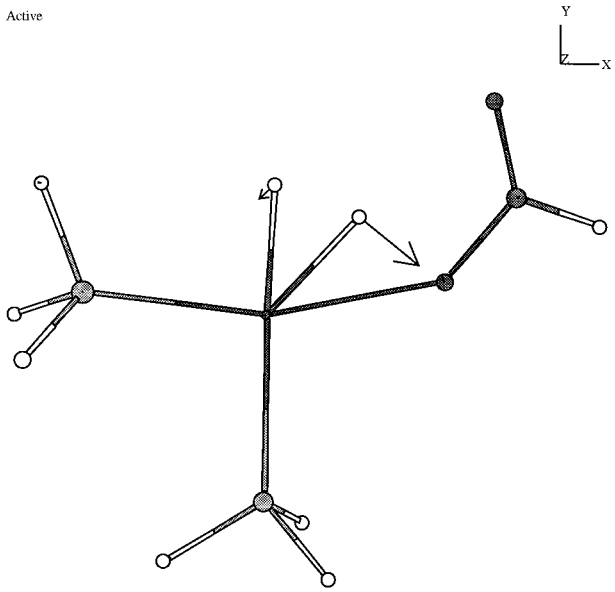

transition state **9** leads naturally to the four-coordinate $[(PH_3)_2Rh(H)(HCO_2H)]$ intermediate **7** that was also the intermediate in the reductive elimination step of the pathway A. Its stabilization with respect to the transition state is computed to be 10.5 and 9.0 kcal mol^{-1} at the MP2//MP2 and QCISD(T)//MP2 levels, respectively. Once **7** has been reached the final part of the catalytic cycle is common to pathways A and B and corresponds to the dissociation of HCO_2H.

The possible existence of a [2 + 2] σ bond metathesis pathway in d^8 transition metal complexes is rather unexpected since this type of reaction is more often associated with early transition metal complexes having low d metal count.[45,46] There is however increasing experimental[47] and theoretical[48] evidence for the occurrence of such processes involving H−H or C−H bonds and late transition metals systems. The key point in these systems is the unsaturation at the metal that is manifested by the presence of a low lying d_σ orbital. In the T-shaped $[(PH_3)_2Rh(HCO_2)]$ system the empty orbital is a hybridized $d_{x^2-y^2}$ orbital interacting in an antibonding way with one of the lone pairs of the bound oxygen atom: see the left side of the schematic orbital interaction diagram of Figure 8. The phase relationship in this orbital is such that it can interact positively with the σ_g orbital of the incoming H_2. On the other hand, the bonding counterpart of $d_{x^2-y^2}$ with the oxygen lone pair, which is doubly occupied and mostly localized on oxygen, will interact positively with $\sigma_u(H_2)$. These two interactions provide already the basis for the allowance of the [2 + 2] reaction.[49] The low magnitude of the energy barrier associated with the transition state **9** results also—and perhaps more crucially—from the presence of a second lone pair on the oxygen atom. This lone

(42) Note that the σ-bond metathesis pathway starting from **4c** and leading to the *cis* HCOOH has a higher energy barrier, 28.1 kcal mol^{-1} (MP2//MP2 value).

(43) A referee suggested a mechanism in which the heterolytic splitting of H_2 would lead to protonation of the formate distal oxygen with hydride addition to the metal center.[44] Such a mechanism would imply to start from **4d** instead of **4b**. Since **4d** is unlikely to be a productive intermediate, this mechanism should not be operative here.

(44) Darensbourg, D. J.; Ovales, C. *J. Am. Chem. Soc.* **1984**, *106*, 3750.

(45) Arndtsen, B. A.; Bergman, R. G.; Mobley, T. A.; Peterson, T. H. *Acc. Chem. Res.* **1995**, *28*, 154 and references therein.

(46) Folga, E.; Woo, T.; Ziegler, T. In *Theoretical Aspects of Homogeneous Catalysis*; van Leeuwen, P. W. N. M., Morokuma, K., van Lenthe, J. H., Eds.; Kluwer: Dordrecht, 1995; p 115 and references therein.

(47) (a) Joshi, A. M.; James, B. R. *Organometallics* **1990**, *9*, 199. (b) Burger, P.; Bergman, R. G. *J. Am. Chem. Soc.* **1993**, *115*, 10462 and references therein. (c) Hartwig, J. F.; Bhandari, S.; Rablen, P. R. *J. Am. Chem. Soc.* **1994**, *116*, 1839. (d) Morris, R. H. *Inorg. Chem.* **1992**, 32, 1471. (e) Lee, J. C.; Peris, E.; Rheingold, A. L.; Crabtree, R. H. *J. Am. Chem. Soc.* **1994**, *116*, 11014. (f) Schlaf, M.; Morris R. H. *J. Chem. Soc., Chem. Commun*. **1995**, 625. (g) Arndtsen, B. A.; Bergman, R. G. Science **1995**, *270*, 1970.

(48) (a) Musaev, D. G.; Mebel, A. M.; Morokuma, K. *J. Am. Chem. Soc.* **1994**, *116*, 10693. (b) Versluis, L.; Ziegler, T. *J. Am. Chem. Soc.* **1990**, *9*, 2985.

(49) (a) Steigerwald, M. L.; Goddard III, W. A. *J. Am. Chem. Soc.* **1984**, *106*, 308. (b) Upton, T. A.; Rappé, A. K. *J. Am. Chem. Soc.* **1985**, *107*, 1206. (c) Jolly, C. A.; Marynick, D. S. *J. Am. Chem. Soc.* **1989**, *111*, 7968.

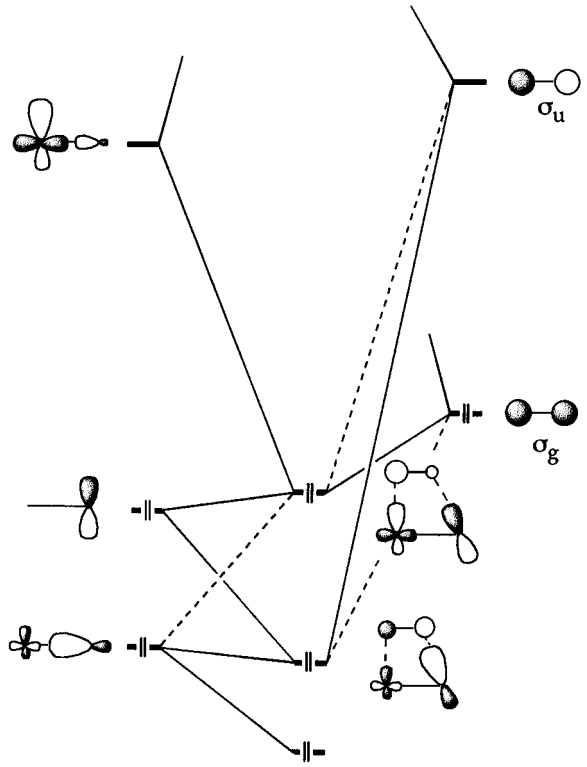

Figure 8. Schematic interaction diagram between the orbitals of $[(PH_3)_2Rh(HCO_2)]$ and the orbitals of H_2 for the transition state of the σ bond metathesis reaction between H_2 and $[(PH_3)_2Rh(HCO_2)]$.

pair is directed toward one incoming hydrogen atom (the one which is of protonic character in the heterolytic splitting of H_2) and can mix with the other orbitals. As a result of this mixing there is a continuous rehybridization throughout the reaction that keeps the best overlap between oxygen and hydrogen.

In fact this situation is symmetric to the one described for early transition metals, *e.g.*, in the [2 + 2] addition of H_2 to $[Cp_2Sc(CH_3)]$.[50] There, a pool of empty s, p, and d orbitals on Sc maintains the optimal overlap with the adjacent ligand orbital. In a more naïve way one could say that in the heterolytic splitting of H_2 that takes place during the [2 + 2] reaction involving early transition metal complexes the empty orbitals on the metal trigger the dissociation of the incipient H^- whereas in the [2 + 2] reaction involving $[(PH_3)_2Rh(HCO_2)]$ the additional lone pair on oxygen triggers the dissociation of the incipient H^+. In that sense this lone pair may be considered to play the same role as an external base.[51−53] It is interesting to note that for the hydrogen exchange in *cis*-$[(PH_3)_4Fe(H)(H_2)]$, which was claimed to take place through an intimate mechanism that is different from the traditional σ bond metathesis,[54] there is no possible involvement of such a lone pair. The same feature also applies to the methane metathesis process at the $[Cp^*Ir(P(CH_3)_3)(CH_3)]^+$ system observed experimentally by Bergman *et al.*[47g] and for which the recent theoretical study of Hall *et al.* points to a two-step oxidative addition/reductive elimination mechanism rather than to a genuine σ-bond metathesis process.[55]

4. Summary and Concluding Remarks

It appears from the present kinetic study that the rate determining step in the hydrogenation of CO_2 catalyzed by bisphosphine rhodium complexes is the product forming step, *i.e.*, the liberation of formic acid from an intermediate that is formed via reversible reactions of the catalytically active intermediate first with CO_2 and then with H_2. Previous NMR investigations provided structural models for possible key intermediates of the catalytic cycle.[5b,7] The *ab initio* calculations, which were based on this sequence, shed more light on the intimate aspects of the mechanism. In particular they suggest an additional hitherto neglected possible pathway for the H_2 activation step that is also consistent with the experimental findings. Our main conclusions on the structural rearrangements for the process leading to the *trans* formic acid are summarized in Figure 9a and the corresponding energy profile is given on Figure 9b.[56] The representation in Figure 9b emphasizes that the σ-bond metathesis pathway provides a much smoother reaction profile than the classical mechanism.

The first step of the catalytic cycle consists of reaction of CO_2 with a neutral rhodium hydride complex which—in analogy to many other catalytic processes involving Rh(I) phosphine complexes[57] and in full agreement with all experimental findings[5b,7,10,11]—is assumed to be a highly unsaturated 14e species $[(P_2)RhH]$. The resulting formate species **4b** corresponds to the intermediate **Rh−1** of eq (f). The calculations show that it can then react with dihydrogen through two fundamentally distinct pathways.[58]

In one case the formate intermediate undergoes a traditional sequence of oxidative addition and reductive elimination reactions (**4b** → **5d** → **6** → **7** → HCO_2H). It appears straightforward in this pathway to specify a dihydrido rhodium (III) formate complex of type **5** as the intermediate **Rh−2** deduced from the kinetic study. According to the calculations the oxidative addition is an easy and quite exothermic process. On the other hand, the reductive elimination appears to be a two step process (**5d** → **7** → HCO_2H) in which a formic acid complex $[(H)(P_2)Rh(HCO_2H)]$ **7** is formed as an intermediate. Formic acid liberation from this complex has an energy demand in the same range as the barrier for hydrogen/formate reductive coupling (**5d** → **6**). Since this coupling is an intramolecular process at the catalytically active center, it would not change the general features of the overall rate law of the catalytic cycle, and **Rh−2** could therefore also correspond to the formic acid complex **7**.

In the alternative pathway (**4b** → **8** → **9** → **7** → HCO_2H), the formic acid complex $[(H)(P_2)Rh(HCO_2H)]$ **7** is formed directly from the formate complex **4b** (*i.e.*, **Rh−1**) via σ-bond metathesis process with a moderate energy barrier, much smaller than the the barrier of the reductive coupling process. Thus **Rh−2** can only be assigned to the formic acid complex **7** in this case. A detailed analysis of the orbital interactions reveals that the presence of an oxygen lone pair of the formate which is not engaged in the bond with rhodium is a prerequisite for the moderate energy barrier.

(50) Ziegler, T.; Folga, E.; Berces, A. *J. Am. Chem. Soc.* **1993**, *115*, 636.

(51) (a) Brothers, P. J. In *Prog. Inorg. Chem. Vol. 28;* Lippard, S. J., Ed.; Wiley: New York, 1981; p 1. (b) Crabtree R. H. In *The Organometallic Chemistry of the Transition Metals (2nd ed.)*; Wiley: New York, 1994; pp 220−221.

(52) Crabtree, R. H.; Lavin, M.; Bonneviot, L. *J. Am. Chem. Soc.* **1986**, *108*, 4032.

(53) Zimmer, M.; Schulte, G.; Luo, X.-L.; Crabtree, R. H. *Angew. Chem.* **1991**, *103*, 206; *Angew. Chem., Int. Ed. Engl.* **1991**, *30*, 193.

(54) Maseras, F.; Duran, M.; Lledos, A.; Bertran, J. *J. Am. Chem. Soc.* **1992**, *114*, 2922.

(55) Strout, D. L.; Zaric, Z.; Niu, S.; Hall, M. B. *J. Am. Chem. Soc.* **1996**, *118*, 6068.

(56) The computed endothermicity of the overall process (1.8 kcal mol^{-1} at the QCISD(T)//MP2 level) is merely the result of considering as a product a monomeric formic acid in the gas phase.

(57) Hofmann, P.; Meier, C.; Englert, U.; Schmidt, M. U. *Chem. Ber.* **1992**, *125*, 353 and references therein.

(58) Note that the corresponding energy values can be influenced by basis set superposition error (BSSE)[59] and zero-point energy corrections. It is difficult to assess BSSE unambiguously,[60] and in a consistent manner,[61] for both pathways. One may reasonably expect, however, that these corrections would be quite similar for both pathways.

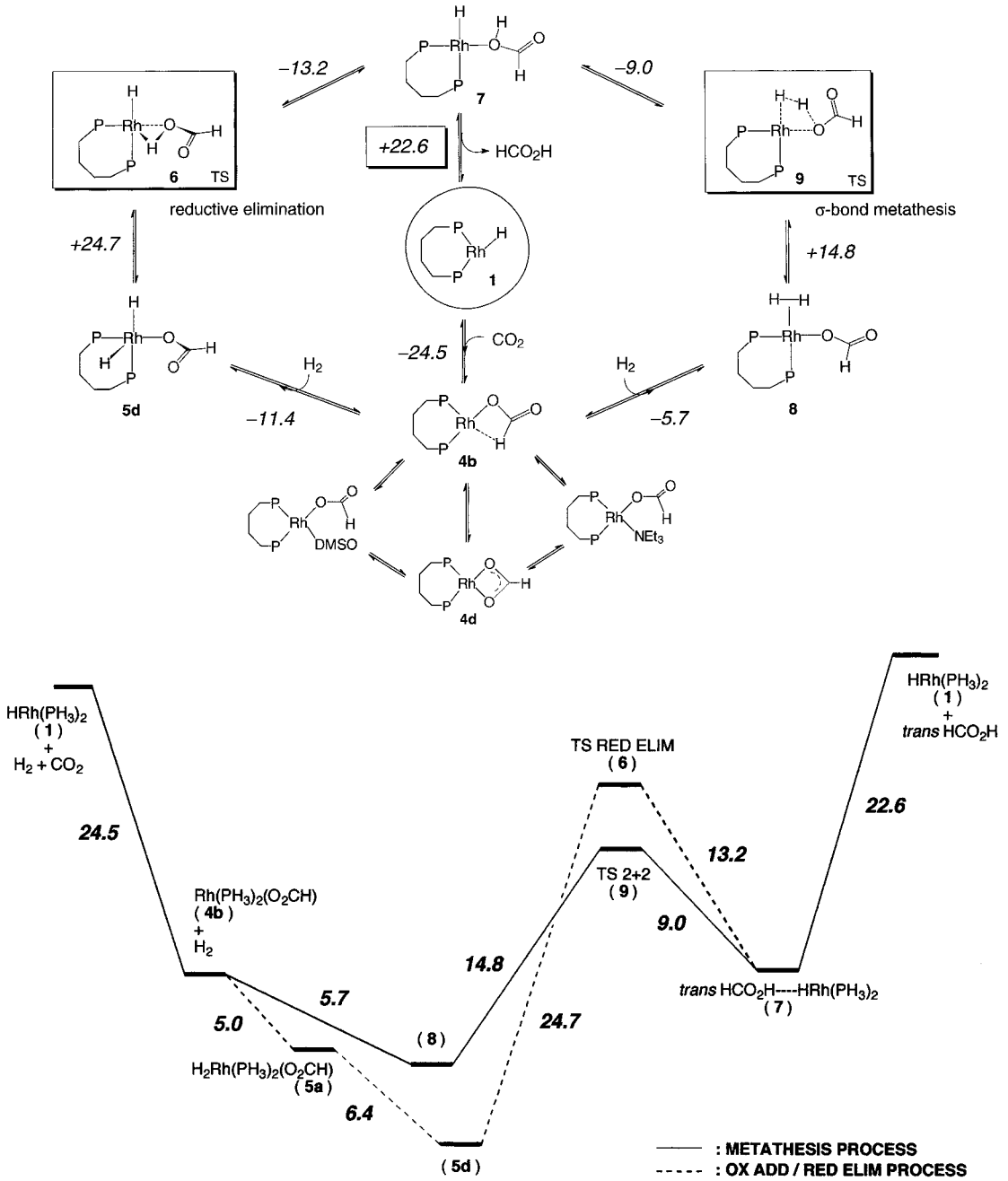

Figure 9. (a) Proposed mechanism for the hydrogenation of CO_2 into *trans*-HCO_2H, catalyzed by bisphosphinehydridorhodium complexes. Energies (in kcal mol^{-1}, at the QCISD(T)//MP2 level) are for the [$(PH_3)_2RhH + CO_2 + H_2$] model system). (b) Energy profiles (at the QCISD(T)//MP2) level for the two alternative pathways. The energies are in kcal mol^{-1}.

At this stage of our investigations it appears appropriate to briefly address an inherent problem of the corroboration of *ab initio* studies with experimental observations in homogeneous catalysis, *i.e.*, the extrapolation of results obtained for gas phase structures to the situation in solution. It is quite clear that donating solvents (such as the DMSO/NEt_3 mixture used in the system under investigation) are capable of filling vacant coordination sites of the highly unsaturated intermediates, as outlined for the formate complexes in the bottom part of Figure 9a.

We are nevertheless confident that the given structures are suitable as a basis for a detailed discussion of the catalytic cycle of CO_2 hydrogenation, as they represent by far the most reactive possible intermediates in all cases where data are available for comparison. Thus we have found a substantially lower barrier for the insertion of CO_2 into the Rh−H bond of [$(PH_3)_2RhH$] than has been reported for the related process involving [$(PH_3)_3$-RhH].[2g] We have also already stressed that three-coordinate Rh(I) complexes appear to be more reactive toward oxidative addition than their four-coordinate counterparts.[30−32] Similar arguments, relying on the lack of catalytic efficiency of highly stable intermediates,[27] have been applied for discarding the η^2-O,O formate complexes **4d** and **5h** as catalytically productive intermediates.

In principle, however, the present solvent system could also interfere with some of the transformations occurring during the catalytic cycle. The presence of the amine might assist the formic acid dissociation by providing alternative pathways, *e.g.*, through an associative mechanism. Furthermore the amine could play a role in the σ-bond metathesis process by acting as an external base.[51] Preliminary results of our calculations indicate that the assistance of the metathesis by an amine can indeed be quite effective.[62] These solvent effects still warrant further theoretical investigations which are presently under way.

5. Experimental Section

5.1. Catalytic Hydrogenation of CO_2. Reagents and General Methodologies. DMSO (fractional distillation under reduced pressure) and NEt_3 (distillation from KOH) were dried, degassed, and stored under argon. Complex **A** was prepared according to ref 6 and crystallized from diisopropyl ether *prior* to use. H_2 (Linde, 5.0) and CO_2 (Linde, 4.8) were used as reaction gases without further purification. ^{1}H-NMR spectra were recorded on a Bruker AC 200 spectrometer operating at 200.13 MHz. The FIDs were transferred to a PC and further analyzed using WINNMR 4.2. ***Caution***: The handling of high pressure equipment, esp. glass apparatus, is hazardous and has to be carried out under appropriate safety conditions.

Kinetic Measurements. The experiments were carried out in a 200 mL stainless steel autoclave equipped with a glass liner, a magnetic stirring barr, and a sampling device.[5b] The reactor was connected to a 500 mL gas reservoir to ensure a practically constant pressure throughout the experiments. The whole system was evacuated and purged with argon three times before each run. The reactor was immersed in a water bath kept at 23 ± 1 °C during reaction. The catalyst solutions were prepared in a Schlenk tube by dissolving the required amount of complex **A** in a mixture of DMSO (10.0 mL) and NEt_3 (2.0 mL) and transferred to the reactor *via* cannula. The reactor was then pressurized with the desired partial pressures of the reaction gases without stirring whereby hydrogen was introduced first except in experiments with CO_2 pretreatment. Reactions were started by switching on the stirrer at a constant stirring rate of 1000 rpm.

Samples of about 0.1−0.2 mL were withdrawn every 3 min within the first 30 min of reaction. The samples were immediately frozen in liquid nitrogen for storage. The frozen samples were diluted with 0.40 mL of a 5:1 mixture of DMSO/[D_6]-DMSO under air to avoid HCOOH decomposition and subsequently analyzed by ^{1}H-NMR spectroscopy (PW = 25% of 90° pulse, RD = 1s, TD = 32 K, RG = 1, NS = 32). The data were subjected to zero filling to 64 K and to exponential multiplication (LB = 0.3) *prior* to Fourier transformation. Formic acid concentrations were determined form the integrals of the signals of the formyl proton at $\delta = 8.34$ and the methyl group of NEt_3 at $\delta = 0.93$ within less than ±5% deviation. Changes in volume owing to the formation of formic acid were neglected.[5b]

Determination of the Relative Solubility of CO_2. An evacuated high pressure NMR tube (Wilmad, 522-PV) containing a mixture of [D_6]-DMSO and amine was pressurized to 1 bar with $^{13}CO_2$ and to a final pressure of 10 bar with $^{12}CO_2$. After gentle activation, the relative solubilities were estimated from the ratio of the ^{13}C signal of dissolved CO_2 ($\delta = 124$) and of the solvent ($\delta = 39.5$) compared to the same ratio in pure [D_6]-DMSO.

6. Computational Details

The BAE(*) basis set is made of a (15, 10, 8) ⟨6, 4, 4⟩ basis[63] for Rh, of the standard (10, 6) and (9, 5) basis sets of Huzinaga[64a] contracted into ⟨4, 3⟩ and ⟨3, 2⟩ for the phosphorus, carbon, and oxygen atoms, respectively. The hydrogen atoms are described by a (4) ⟨2⟩ basis set.[64b] Polarization functions (of exponent 0.63, 1.33, and 0.8 respectively) are added to the C, O, and the H atoms taking an active part of the catalytic process (*i.e.*, the hydrogen atoms originating from H_2 and the hydride of the [$HRh(PH_3)_2$] system). The geometry optimizations were carried out with the six cartesian d functions. Crucial points (in particular the transition states) were characterized by a frequency analysis performed analytically for the insertion step and numerically for the other steps. The geometry optimizations were followed by single point energy calculations carried out at the MP2 and at the QCISD(T) level, using five functions with true d character and the frozen core approximation. The corresponding total energies of the various structures are given in Table 3.

Acknowledgment. Financial support by the Max-Planck-Society, the CNRS, and the Fonds der Chemischen Industrie is gratefully acknowledged. Additional support from a French−German PROCOPE contract (No. 94132) made the close cooperation possible. We also thank Degussa AG for a loan of $RhCl_3 \times 3H_2O$. Calculations were carried out on the IBM RS 6000 workstations of our laboratory, of the Institut du Developpement et de Ressources en Informatique Scientifique (IDRIS, Orsay), and on the DEC 3000/600S workstations of the Centre Universitaire Régional de Ressources Informatiques (CURRI, Strasbourg). We thank the staffs of these two centers for their cooperation. A.D. and F.H. are grateful to Dr. L. Padel and Mrs. Fersing for their help and technical assistance. W. L. wishes to thank Prof. E. Dinjus, Jena, for his support and Prof. G. Fink, Mülheim, for helpful and stimulating discussions.

JA961579X

(59) van Duijneveldt, F. B.; van Duijneveldt-van de Rijdt, J. G. C. M.; van Lenthe, J. H. *Chem. Rev.* **1994**, *94*, 1873.

(60) Parasuk, V.; Almlöf, J.; DeLeeuw, B. *Chem. Phys. Lett.* **1991**, *176*, 1.

(61) Davidson, E. R.; Chakravorty, S. J. *Chem. Phys. Lett.* **1994**, *217*, 48.

(62) Hutschka, F.; Dedieu, A. *J. Chem. Soc., Dalton Trans.* in press.

(63) Veillard, A.; Dedieu, A. *Theor. Chim Acta* **1984**, *65*, 215. The original (15, 9, 8) basis set was modified by the addition of a p function of exponent 0.15.

(64) (a) Huzinaga, S. *Technical Report*; University of Alberta, Edmonton, 1971. (b) Huzinaga, S. *J. Chem. Phys.* **1965**, *42*, 1293.